Supporting Information

Aggregation in a High Mobility n-type Low Bandgap Copolymer with Implications on Semicrystalline Morphology

Robert Steyrleuthner[1], Marcel Schubert[1], Ian Howard[2], Bastian Klaumünzer[3], Kristian Schilling[4], Zhihua Chen[5], Peter Saalfrank[3], Frédéric Laquai[2], Antonio Facchetti[5] and Dieter Neher[1]

[1]*University of Potsdam, Institute of Physics and Astronomy, Germany*
[2] *Max Planck Institute for Polymer Research, Mainz, Germany*
[3]*University of Potsdam, Institute of Chemistry, Germany*
[4] *Nanolytics GmbH, Potsdam, Germany*
[5]*Polyera Corporation, Illinois, USA*

Experimental

For solution spectra, the polymer was dissolved in toluene, chlorobenzene, chloroform (typical purities of 99,9%), 1,2-dichlorobenzene, 1,2,4-trichlorobenzene (purities min. 99%) and 1-chloronaphthalene (>85 %, remainder 2-chloronaphthalene). All solvents were obtained from Sigma-Aldrich. For optical investigations on P(NDI2OD-T2) layers, solutions were spin coated directly on glass.

Steady-state spectroscopy:
Absorption measurements of solutions (filled in quartz cuvettes) and thin films have been carried out with a Varian Cary 5000 UV-VIS-NIR absorption spectrometer. Fluorescence measurements were performed by exciting the samples with a wavelength tunable DPSS laser (Ekspla NT242) and detecting the photoluminescence with an Andor iDus DU420A CCD camera attached to a Shamrock 303i spectrograph, while the light was coupled in via an optical fiber. In order to prevent filter effects, a face-on geometry and thin 1 mm cuvettes were used. Appropriate glass color filters were used in order to repress the second order of the laser excitation appearing in the spectra. Excitation spectra were recorded using a Horiba Jobin-Yvon Fluorolog 3 spectrofluorometer.

NMR Spectroscopy:
The NMR spectra were recorded on a Mercury 400 (400 MHz) spectrometers at the setting temperatures, and chemical shifts are referenced to residual protio-solvent signals. The NMR sample concentration was 15 g/l.

Analytical Ultracentrifugation:
Viscosities of the solvent mixtures have been determined with a Haake Rheo Stress Rheometer RS 150. The corresponding densities have been measured using a Anton Paar density meter DMA 4500. Analytical Ultrancentrifugation experiments were conducted on a BeckmanCoulter Optima XL-A/XL-I instrument, applying absorbance detection at various wavelengths. An angular velocity of 40000 rpm was chosen for sedimentation velocity experiments, including such under density variation, sedimentation equilibrium was attained after five days at 10000 and 14000 rpm. All experiments were carried out at 20°C. The samples were investigated in cells equipped with titanium centrepieces and sapphire windows.

Transient Absorption and Streak Camera:
Fluorescence lifetime measurements were performed using a Streak Camera System (Hamamatsu C4742) after excitation by the frequency doubled output of a Ti:Sapphire laser oscillator (Mira, Coherent Inc.). Transient absorption experiments were performed using a regenerative amplifier (Libra, Coherent Inc.: 1 kHz, 3.5W, 800 nm). Excitation pulses were generated either by doubling a portion of the fundamental beam or by using an optical parametric amplifier (OPerA Solo, Light Conversion Inc.) and chopped to 500 Hz mechanically. The probe pulse was generated by single filament super-continuum generation in a sapphire plate. The probe beam was detected by dispersion onto a linear detector by a spectrograph; every pulse was read into a PC to calculate ΔT/T.

Solvent Properties

Name	Polarizability α [10^{-24}cm^3]	Boiling Point [°C]
toluene	11.8	110.63
chlorobenzene	14.1	131.72
chloroform	9.5	61.17
1,2 - dichlorobenzene	14.2	180
1,2,4-trichlorobenzene	16.3	213.5
1-chloronaphthalene	19.3	259

from "CRC Handbook of Chemistry and Physics" 87th Edition, 2006

Excitation Spectra

In toluene the excitation spectrum of the minor emission at 710 nm is caused by the absorption also seen in CN. Also, the dominating long wavelength emission in toluene is generated undoubtedly by a second absorption feature peaking at 720 nm. This suggests that the polymer in toluene exists in at least two distinct states with characteristic absorption and emission. We note that the PL in toluene differs slightly from the spectrum presented in Figure 1b due to a lower polymer concentration used here (see Figure S2 for details).

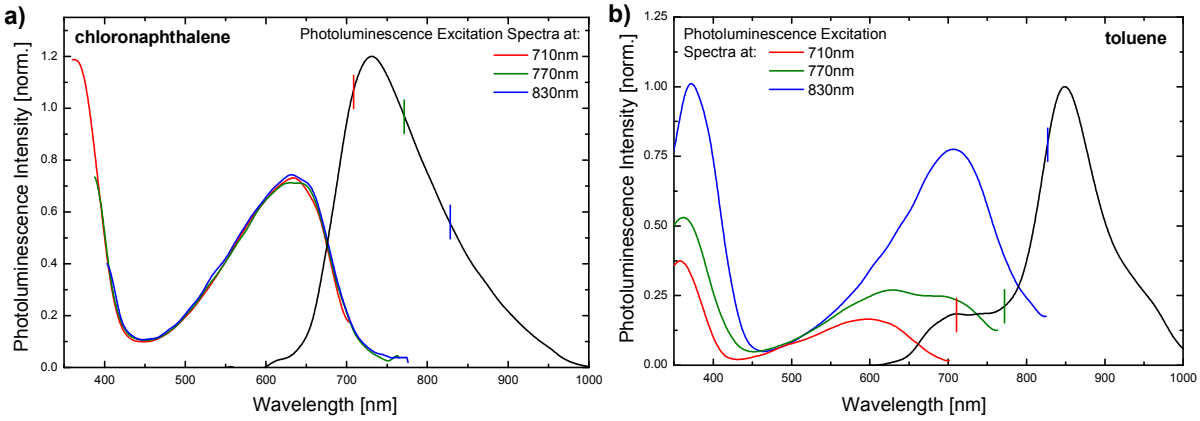

Figure S1 *Excitation spectra of P(NDI2OD-T2) in chloronaphthalene (a) and in toluene (b) at a concentration of 0.01 g/l. Excitation spectra have been recorded for emission at 710 nm, 770 nm and 830 nm (as indicated in the PL spectra).*

Concentration Dependence of Absorption and PL in Toluene

In figure 3b we show, that the absorption of P(NDI2OD-T2) in various solvents does not depend on the polymer concentration over several orders. However, although this change does not induce new states which would occur in absorption, close proximity of the chains can enhance the transfer of excitons to the lowest excited state (aggregate emission). Therefore decreasing the concentration enhances the emission of the amorphous chains slightly.

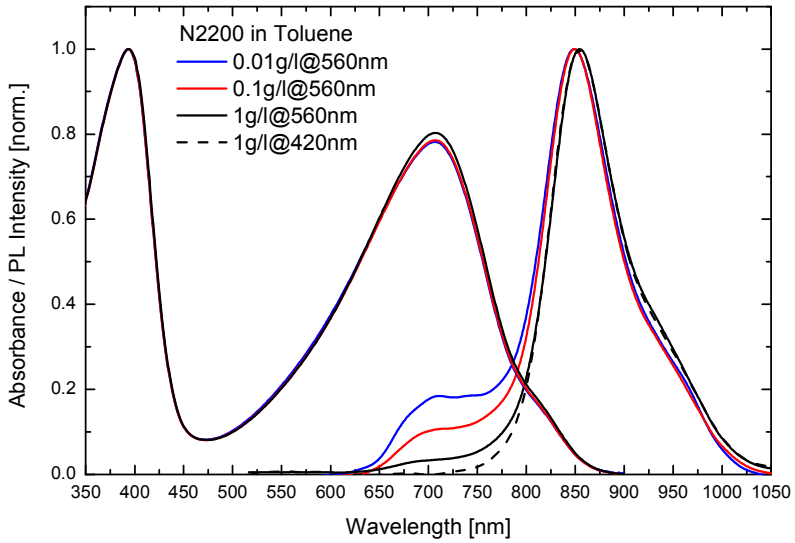

Figure S2 *Absorption and fluorescence spectra of P(NDI2OD-T2) at various concentrations in toluene. The PL spectra were recorded for an excitation wavelength of 560 nm and 420 nm as indicated in the graph.*

Quantum Chemical Calculations

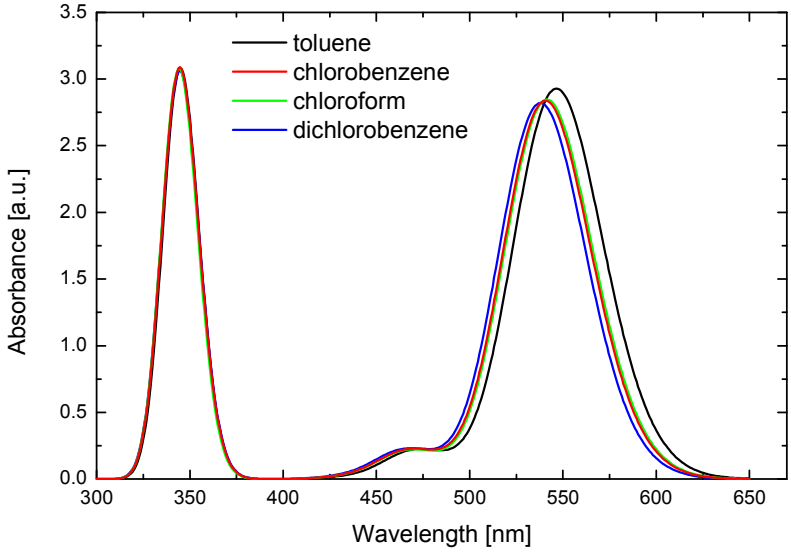

Figure S3 *Calculated absorption (TD-CAM-B3LYP/SVP) for a P(NDI2OD-T2) trimer (broadened in energy by σ=100meV) placed in different solvent shells (via PCM field approach.)*

NMR Atom Assignment

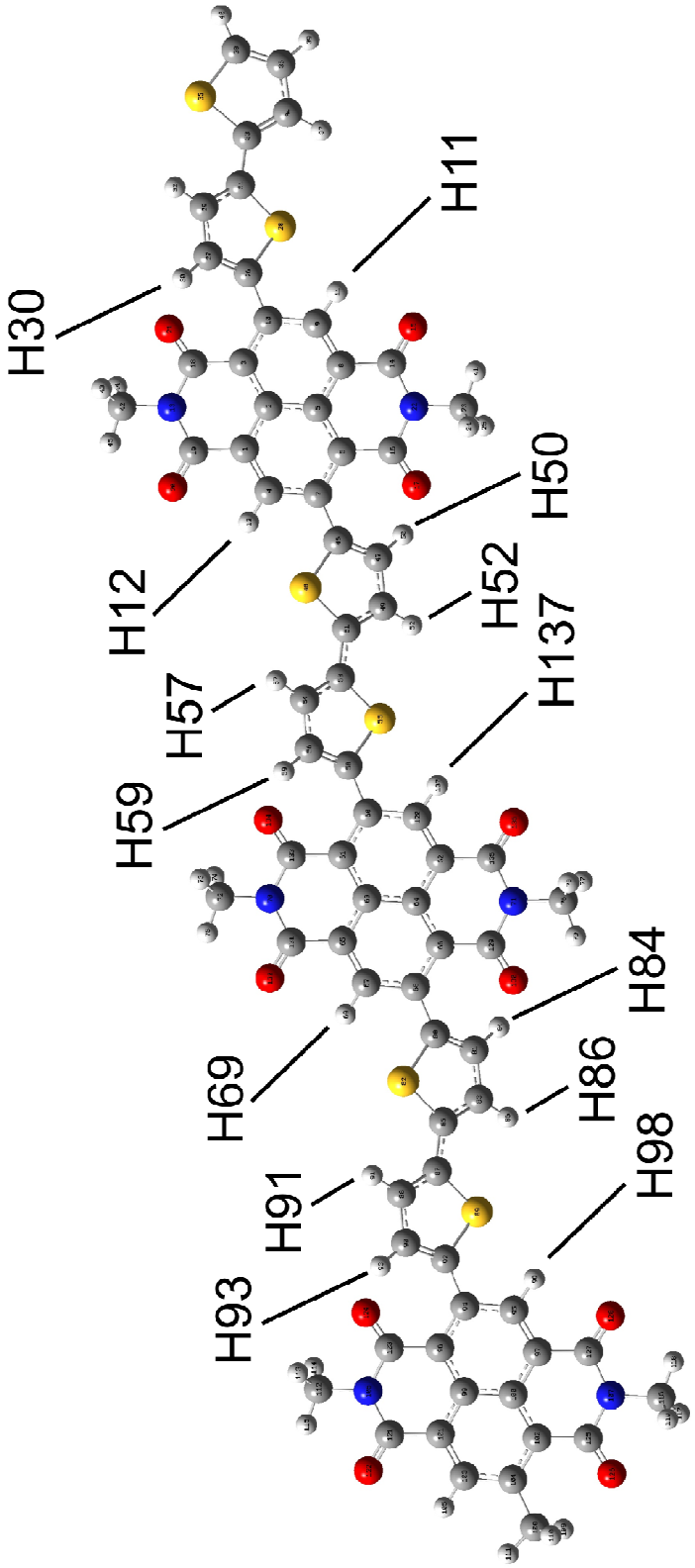

Figure S4 *DFT optimized structure* (B3LYP-SVP) *of a single P(NDI2OD-T2) trimer. The atom numbering corresponds to the chemical shifts shown in Figure 5a in the main text.*

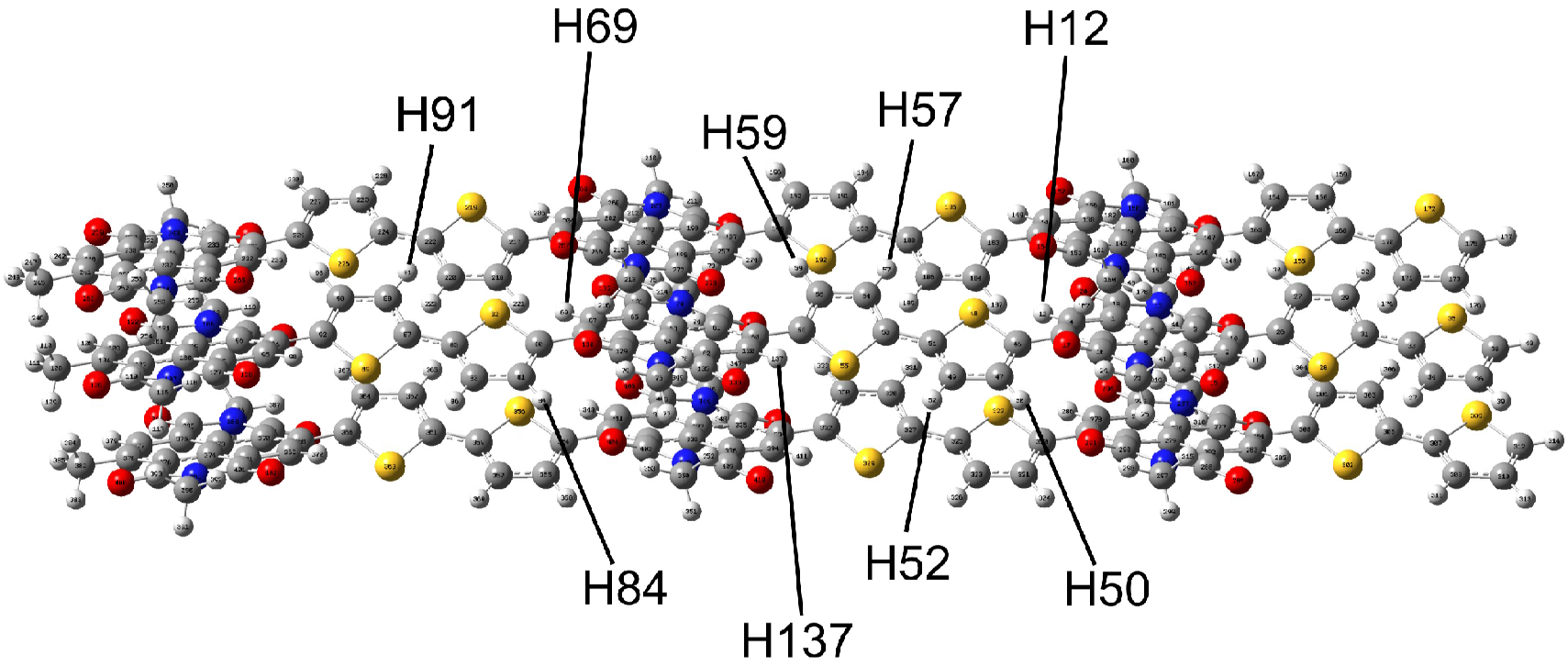

Figure S5 *P(NDI2OD-T2) triple-stack constructed by using two stacked and DFT optimized trimers (*B3LYP+D2/SVP). *The third trimer was placed on top* using the geometric displacement of the NDI units in the optimized stack

Decomposition of the Optical Spectra

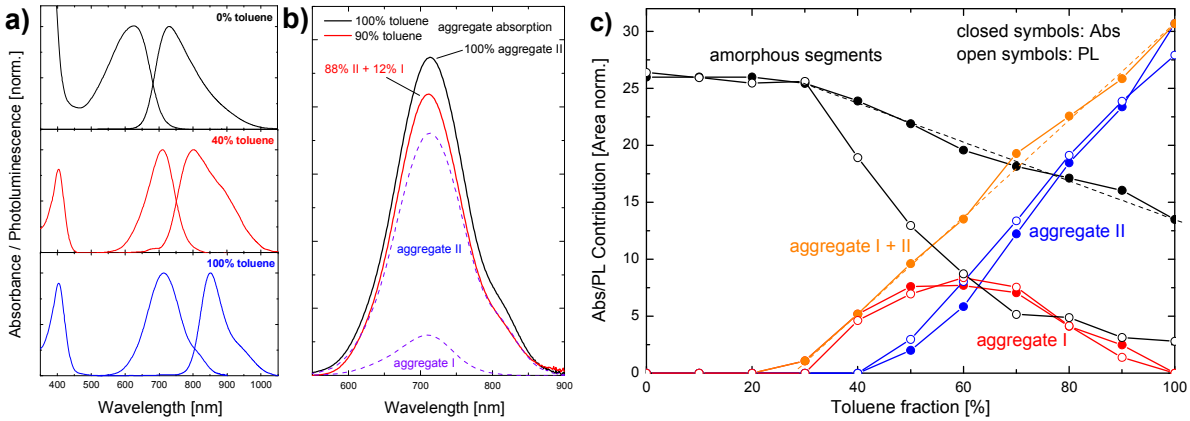

Figure S6 *a) Absorption and emission of the intrachain exciton (0% toluene), intermediate aggregate I (40% toluene) and aggregate II (100% toluene). Spectra of the pure species are gained by subtraction the contributions from the two other species as described in the text. b) Aggregate absorption in 100% and 90% toluene (black and red line) gained by subtraction of the intrachain exciton absorption. The dotted lines also show the contributions of the two aggregate species to the 90% toluene absorption. c) Integral contributions of the different species to absorption (absolute) and emission (scaled).*

To address the issue of aggregate species in greater detail, the absorption and emission spectra were decomposed into contributions from all three species (Figure S6a). The fluorescence in 100% toluene is determined by primarily from aggregate II with a small contribution from the intrachain exciton and no sign of aggregate I. We then make the assumption that absorption (comprising absorption at 710 nm and 815 nm) in 100% toluene is also entirely caused by aggregate II (Figure S6b); this assumption as justified in the main document. The absorption at lower toluene content can be then be fit as a superposition of three components. One component is that of the aggregate II absorption just determined. The second component is that of un-aggregated chromophores, whose spectrum is known from the 100% CN solution. Finally, there is a component due to aggregate I. We find aggregate I's spectrum by first subtracting the absorption of the unaggregated chromophores from all spectra. Subsequently the absorption spectrum of the 100% toluene mixture is scaled and subtracting from the 90% toluene mixture in order to leave only the contribution of aggregate I to the 90% mixture's absorption spectrum. This process is detailed in Figure S1b, and the absorption of aggregate I is found to be a single band peaking at 710 nm. This spectrum we obtain for aggregate I is identical to the absorption spectrum in the 40% toluene mixture, consistent with our observation based on the photoluminescence that first aggregate I forms, and then is replaced by aggregate II. We quantify this behavior by fitting each absorption spectrum to a superposition of these three components. This allows us to quantify the fraction of the absorption from unaggregated chromophores, and chromophores in the aggregate I and aggregate II states that we show in Figure 9c as solid symbols.

We then perform a similar analysis on the fluorescence spectra. The fluorescence of the intrachain exciton and aggregate II were taken directly from the 0% (excitation 560 nm) and 100% toluene spectra (excitation 420 nm) respectively. Then, the emission spectrum of the intermediate aggregate I was gained by subtracting these two contributions from the spectra in mixed solvents (Figure S6a). The integrated contributions of the three species to the overall fluorescence are plotted in Figure S1c as a function of toluene content. Since the quantum

efficiencies and transfer rates between the particular species are not known, the integrated contributions for each species derived from fluorescence spectra have been scaled independently to match the contributions from the deconvolution of the absorption spectra at their respective maxima.

These contributions by chromophores in aggreagate I and aggregate II states to the photoluminescence compare well to the relative contributions elaborated from the absorption spectra. The intermediate appearance of the aggregate I PL directly relates to the presence of the 710 nm single peak in the absorption analysis presented in Figure 6. However, the contribution by the non-aggregated chains to the photoluminescence is significantly less than its contribution to the absorption when the chains start to aggregate above 30% toluene content. This suggests that energy transfer from the exciton residing in the non-aggregated chomophores to both aggregate I and aggregate II in the aggregated region can occur. Given the significant overlap between the exciton emission and the aggregate absorption this is not surprising. Interestingly, that the sum of the aggregate contributions in absorption appears to increase continuously and linearly with toluene content, without a visible change in the slope, suggesting that aggregate II is formed by replacing the intermediate aggregate I, and that aggregate I has completely disappeared in 100% toluene.

Solution Time resolved Spectroscopy Fitting

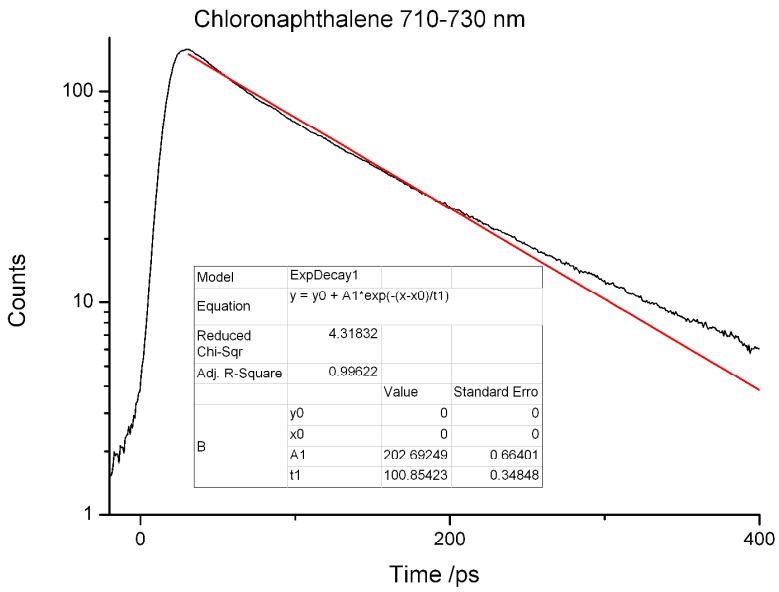

Figure S7 *Fit of the P(NDI2OD-T2) emission in chloronapthalene showing that the unquenched intrachain exciton lifetime is approximately 100 ps. The lifetime is non monoexponential likely due to spectral diffusion caused by relaxation of the excited states within the density of states.*

The kinetics of the fluorescence decay in the CN:toluene solution are simultaneously fit at 710-730 nm and at 770-790 nm. In both wavelength regions both exciton emission and Agg I emission are observable, however from 710-730 nm the exciton emission is dominate while from 770-790 nm the Agg I emission is dominant.

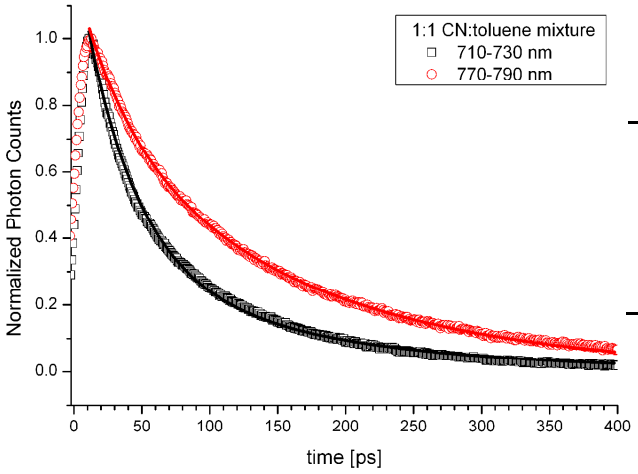

	710-730 nm	770-790 nm
A1 (±.01)	0.42	0.87
A2 (±.01)	0.91	0.32
t1 /ps	156 ± 1	
t2/ps	32 ± 1	

Figure S8 *A biexponential function is fit simultaneously to both wavelength regions, with the decay constants shared but the amplitudes individually fitted. This approach allows the faster rate of (quenched) exciton decay, and the slower rate of Agg I decay to be extracted as 32 and 156 ps respectively. The full set of extracted parameters are shown in the Table to the rigth.*

Analytical Ultracentrifugation

Density Variation Experiment

As these toluene and toluene-d_8 can be considered as chemically identical solvents, the addition of the more dense toluene-d_8 to normal toluene shall neither change the particle diameter nor induce particle agglomeration. Under these presumptions, the only parameter that is varied between these two sedimentation experiments is the solvent density and viscosity, leading to a difference in the measured sedimentation coefficient. Therefore, the dry density can be determined from two sedimentation experiments with chemically identical solvents but different density and viscosity free of further assumptions.For each datapoint of the sedimentation coefficient distribution, a partial specific volume for the species represented by this datapoint is calculated by[1]

$$\bar{v} = \frac{\eta_1 s_1 - \eta_2 s_2}{\eta_1 \rho_2 s_1 - \eta_2 \rho_1 s_2} \quad \text{(S1)}$$

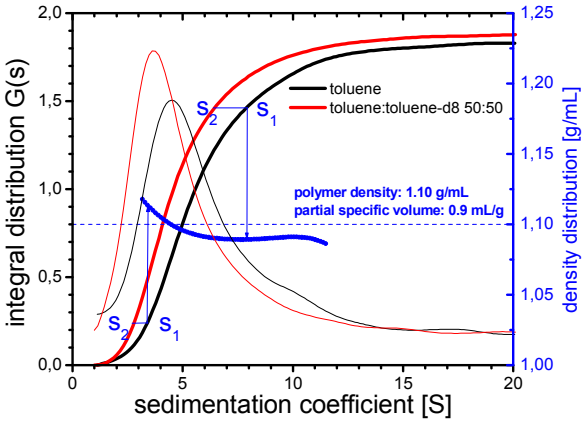

Figure S9 *Sedimentation coefficient distribution G(s) of P(NDI2OD-T2) in toluene and toluene:toluene-d_8 mixture. Also shown is the differential distribution g(s). The dry density around the maximum of the distribution is found to be 1.1 g/mL, decreasing to higher sedimentation coefficients. The blue arrows indicate corresponding pairs (s1,s2) with same G(s) value, computed to yield the local density for this species.*

We find the polymer dry density to be slightly inhomogeneous, decreasing towards higher molecular masses. For all further calculations, we accept the value of 0.9 mL/g in the maximum of the sedimentation coefficient distribution as a reasonable average.

Equilibrium Experiments

For evaluation, only the particle dry density ρ_P and the solvent density ρ are required. The simplest approach for the calculation of M_w is the thermodynamically derived equation[2]

$$M = \frac{2 N_A k_B T}{\left(1 - \bar{v}\rho\right)} \times \frac{d \ln c}{d r^2}, \qquad \text{(S2)}$$

where c ist the particle concentration determined here by absorption measurements over the radial coordinate of the sedimentation cell in equilibrium. Thus, a plot of $ln(c)$ vs. r^2 shows a straight line, the slope being proportional to the molecular mass. Multiple species produce a sum of exponential concentration profiles; the plot of ln(c) over r^2 will then not exhibit straight lines with constant slope but will bent as higher molecular weight coils or agglomerates will accumulate closer to the cell bottom. This case is given for the present material which is highly polydisperse (Figure SX). Averaging the local values for M over the entire cell range yields the mass averaged molecular mass M_w.[3] Though more sophisticated methods of evaluation exist (such as model dependent fits or the M* function suggested by Creeth and Harding),[4,5] we chose the simple approach for evaluation as this is the best option for polydisperse systems.

The angular velocity was chosen such that the concentration profiles extended over the entire cell range, but allowing for depletion of the polymer at the meniscus. After five days, absorption scans were taken at 500 nm and 710 nm.

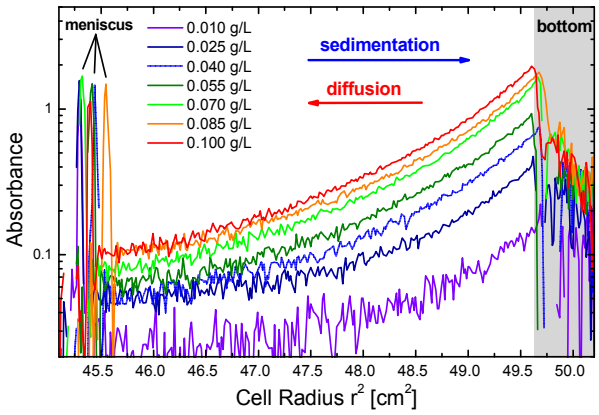

Figure S10 *AUC equilibrium concentration profiles of P(NDI2OD-T2) in pure toluene at various concentrations probed at 710 nm.*

Frictional Ratio

The frictional ratio f/f_0 is the ratio of sedimentation coefficient of the theoretical compact sphere and the actual object and can be calculated from the measured sedimentation coefficient if the molecular mass is known:

$$\frac{f}{f_0} = \frac{s_{compact}}{s_{measured}} = \frac{M\left(1-\bar{\nu}\rho\right)}{N_A\, 6\pi\eta\, s_{measured}} \times \left(\frac{4\pi N_A}{3\bar{\nu}M}\right)^{1/3} \quad \text{(S3)}$$

Transient Absorption on CN:CF Films

As shown in Figure S12, the annealed film shows a clear bleach peak at approximately 790 nm corresponding to the unique peak observed in the steady state absorption caused only by aggregate II (Figure 7 main text). With time, the absorption bleach red shifts, consistent with diffusion of the excited-state species to lower lying energy levels in the broadened density of states. This spectral diffusion is also consistent with quenching of the emission lifetime due to diffusion to quenching sites. In the as prepared film, the shoulder at 800 nm is much less clear, and only visible at later times. This suggests that aggregate I species dominate the population of the as prepared film directly after photoexcitation, and as time progresses some fraction of these excitations transfer their energy to the aggregate II species. At late times these lower energy aggregate II states form a significant fraction of the remaining excited-state population, as seen by the extension of the absorption bleach to 800 nm after approximately 200 ps. However, the emission from aggregate I states observed in the time resolved emission experiment demonstrates that transfer to aggregate II does not quench all aggregate I states.

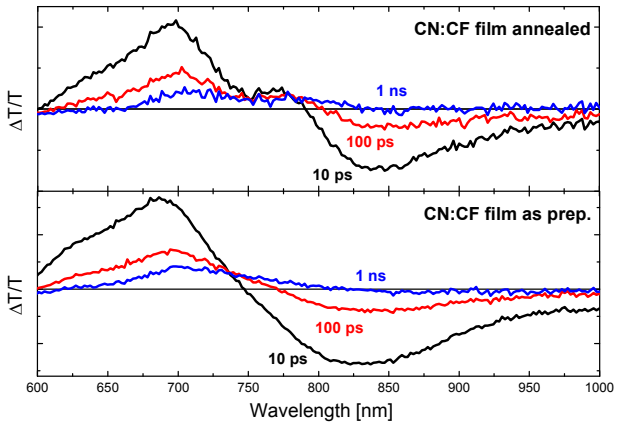

Figure S12 *Transient absorption spectra at various time delays after 530 nm excitation for annealed and as prepared films cast from chloronaphthalene:chloroform solvent mixture.*

We note that a significant fraction of the absorption bleach remains even after 2.5 ns, while no emission can be seen as judged from the streak camera measurements and the photoinduced absorption in the 850-1000 nm wavelength region is negligible. These observations suggest that some fraction of the photoexcitaitons are converted into long-lived nonemissive species such as triplets or charges. The ratio between the initial and long-lived signal is similar in the annealed and as prepared films, so it appears that the formation of long-lived states is not affected by the film annealing. Similar initial to long-lived absorption ratios were observed for amorphous polythiophene films and assigned to triplets,[6] so partial intersystem crossing into a triplet population on this timescale in P(NDI2OD-T2) is not unreasonable, however further work is necessary to firmly assign the population responsible for the long-lived absorption bleach.

(1) Schilling, K. *PhD Thesis, University Potsdam* **1999**.

(2) Svedberg, T.; Pedersen, K. O. *Angewandte Chemie, Steinkopff Verlag* **1940**, *53*, 195.

(3) Elias, H. G. *Makromoleküle, Hüthig & Wepf, Basel* **1990**.

(4) Creeth, J. M.; Harding, S. H. *Journal of Biochemical and Biophysical Methods* **1982**, *7*, 25.

(5) Cölfen, H.; Harding, S. E. *Eur. Biophys. J. Biophys. Lett.* **1997**, *25*, 333.

(6) Howard, I. A.; Mauer, R.; Meister, M.; Laquai, F. d. r. *Journal of the American Chemical Society* **2010**, *132*, 14866.